Validation of empirical and semi-analytical remote sensing algorithms for estimating absorption by Coloured Dissolved Organic Matter in the Baltic Sea from SeaWiFS and MODIS imagery*

OCEANOLOGIA, 52 (2), 2010.
pp. 171–196.

© *2010, by Institute of Oceanology PAS.*

KEYWORDS
Remote sensing
Ocean colour
Satellite validation
SeaWiFS
MODIS
Coloured dissolved organic matter
Absorption

Piotr Kowalczuk⋆
Mirosław Darecki
Monika Zabłocka
Izabela Górecka

Institute of Oceanology,
Polish Academy of Science,
ul. Powstańców Warszawy 55, PL–81–712 Sopot, Poland;

e-mail: piotr@iopan.gda.pl

⋆corresponding author

Received 18 November 2009, revised 7 April 2010, accepted 12 April 2010.

Abstract

An extensive bio-optical data set obtained from field measurements was used to evaluate the performance of an empirical (Kowalczuk et al. 2005) and two semi-analytical algorithms: Carder et al. (1999) and GSM01 (Maritorena et al. 2002) for estimating CDOM absorption in the Baltic Sea. The data set includes coincident measurements of radiometric quantities and absorption coefficients of CDOM made

* This paper was presented at the Remote Sensing and Water Optics Workshop of the 7th Baltic Sea Science Congress, August 2009, Tallinn, Estonia.

This study was funded by Statutory Research Programme No. II.5 at the Institute of Oceanology, Polish Academy of Sciences, Sopot, Poland and by research grant No. N N306 2942 33 awarded to PK by the Polish Ministry of Science and Higher Education.

The complete text of the paper is available at http://www.iopan.gda.pl/oceanologia/

during 43 cruises between 2000 and 2008. In the first stage of the analysis, the accuracy of the empirical algorithm by Kowalczuk et al. (2005) was assessed using in situ measurements of remote sensing reflectance. Validation results improved when matching points located in Gulf of Gdańsk close to the Vistula River mouth were eliminated from the data set. The calculated errors in the estimation of $a_{\mathrm{CDOM}}(400)$ in the first phase of the analysis were $Bias = -0.02$, RMSE = 0.46 and $\mathrm{R}^2 = 0.70$. In the second stage, the empirical algorithm was tested on satellite data from SeaWiFS and MODIS imagery. The satellite data were corrected atmospherically with the MUMM algorithm designed for turbid coastal and inland waters and implemented in the SeaDAS software. The results of the best case scenario for estimating the CDOM absorption coefficient $a_{\mathrm{CDOM}}(400)$, based on SeaWiFS data, were $Bias = -0.02$, RMSE = 0.23 and $\mathrm{R}^2 = 0.40$. The validation of the Kowalczuk et al. (2005) empirical algorithm applied to MODIS data led to a less accurate estimate of $a_{\mathrm{CDOM}}(400)$: $Bias = -0.03$, RMSE = 0.19 and $\mathrm{R}^2 = 0.29$. This assessment of the accuracy of standard semi-analytical algorithms available in the SeaWiFS and MODIS imagery processing software revealed that both algorithms (GSM_01 and Carder) underestimate CDOM absorption in the Baltic Sea with mean systematic and random errors in excess of 70%. The paper presents examples of the application of the Kowalczuk et al. (2005) empirical algorithm for producing maps of the seasonal distribution of $a_{\mathrm{CDOM}}(400)$ in the Baltic Sea between 2004 and 2008.

1. Introduction

CDOM is the primary absorber of sunlight and a major factor determining the optical properties of Baltic Sea waters. It also affects directly both the availability and the spectral quality of light in aquatic environments. The absorption of light by CDOM influences both the inherent and apparent optical properties of seawater. CDOM absorption, together with light absorption by pure water, phytoplankton pigments, organic and inorganic matter suspended in marine waters, and also light scattering, shapes the spectral optical properties of sea water and the light field in the water column (Morel & Prieur 1977, Sathyendranath (ed.) 2000, Blough & Del Vecchio 2002). For this reason, the optical properties of CDOM have been an object of study since the inception of ocean optics as a marine science discipline (Jerlov 1976). CDOM absorption decreases exponentially towards longer wavelengths and can be described by the exponential equation (Kirk 1994)

$$a_{\mathrm{CDOM}}(\lambda) = a_{\mathrm{CDOM}}(\lambda_0)e^{-S(\lambda-\lambda_0)}, \tag{1}$$

where $a_{\mathrm{CDOM}}(\lambda)$ is the absorption coefficient at wavelength λ, λ_0 is the reference wavelength, and S is the slope coefficient (the exponential decrease of the absorption spectrum over a given wavelength range). These parameters describe CDOM quantitatively and can be used to estimate

the entire absorption spectrum from equation (1) if absorption at the fixed (reference) wavelength and S are known.

Interest in CDOM and its characterisation has increased recently for several reasons: i) remote sensing of ocean colour, related to organic carbon cycling; ii) remote sensing of chlorophyll a as an indicator of primary productivity and the potential interference in its measurement due to CDOM; iii) air-sea exchange of important trace gases, namely CO, CO_2 and COS; iv) the formation of reactive oxygen species and their potential impact on biological processes and geochemical cycling; v) as a tracer of riverine input of organic carbon to the ocean and carbon cycling in coastal waters; vi) attenuation of ultraviolet light in surface waters. Through its effects on underwater solar radiation, CDOM can either stimulate or hinder biological activity (e.g. Mopper & Kieber 2002). In coastal waters in particular, quantitative descriptions of the dynamics and variability of CDOM optical properties are often required in order to accurately predict light penetration and consequently, such parameters as primary productivity.

Another area in which quantitative and qualitative assessments of CDOM optics are important is remote sensing (Siegel et al. 2002, Blough & Del Vecchio 2002). Semi-analytical algorithms for estimating the inherent optical properties of sea waters from ocean colour satellite imagery produce values of chlorophyll concentrations together with CDOM and particulate absorption coefficients (Garver & Siegel 1997, Maritorena et al. 2002). These algorithms were applied to produce maps on a basin scale, as well as of the global distribution of CDOM absorption and its seasonal variability (Siegel et al. 2002). The application of semi-analytical algorithms to observations of CDOM absorption by ocean colour imagery has also led to an explanation of the differences in chlorophyll a retrievals resulting from the application of empirical algorithms in various oceanic basins (Siegel et al. 2005b), and hence a reassessment of the principal theoretical assumptions of ocean optics (Siegel et al. 2005a). In oceanic coastal areas and semi-enclosed seas, which are optically complex case 2 waters, empirical band ratio algorithms are often used to estimate CDOM absorption and its impact on light transmission through the water column in the UV and visible spectrum (Kahru & Mitchell 1999, Kahru & Mitchell 2001, D'Sa et al. 2002, D'Sa & Miller 2003, Johannessen et al. 2003, Fichot et al. 2008, Mannino et al. 2008).

The application of ocean colour remote sensing to estimate CDOM optical properties together with models of their modification through photochemical reactions (Johannessen & Miller 2001) has provided an opportunity to study CDOM mineralisation over vast areas of oceans basins (Bélanger et al. 2006, Del Vecchio et al. 2009). These studies contribute

directly to carbon cycle research calculations of CO_2 exchange between the ocean and the atmosphere. CDOM is part of the DOM pool, which represents the largest reservoir of organic carbon in the oceans. About 97% of all organic carbon in the sea is bound up in DOM, with an estimated 685 Gt as dissolved organic carbon (DOC) (Hansell & Carlson 2001). In those marine waters where there is a high correlation between CDOM and DOC concentrations, CDOM can be a proxy for DOC concentration. Although there is no universal relationship between the CDOM absorption coefficient and DOC concentration, there are examples of remote sensing techniques being applied to the study of DOC dynamics in the coastal waters of oceans (Del Castillo & Miller 2008, Mannino et al. 2008).

The Baltic Sea has high concentrations of CDOM as a result of the large input of fresh water from its extensive drainage basin and limited water exchange with the North Sea. The optical effects of CDOM are, therefore, particularly relevant in this area. The southern Baltic Sea is located in the temperate climatic zone. Maximum freshwater runoff occurs in April/May and coincides with the spring phytoplankton bloom that is initiated by the stabilisation of the water column and increased surface light. The fresh water carries with it both high concentrations of CDOM and a substantial load of inorganic nutrients. The nutrients enhance the spring bloom, and, combined with the CDOM, cause an increase in light attenuation. In the summer, local coastal upwelling caused by Ekman transport and periodic summer floods affect the optical properties in the coastal zone and bays. In the winter, wind-driven mixing, vertical thermohaline circulation, decreased biological activity and reduced riverine outflow all resulted in clearer surface waters (Sagan 1991, Olszewski et al. 1992, Kowalczuk 1999). CDOM has a significant influence on the spectral properties of the apparent optical properties of Baltic Sea water. High CDOM concentrations in the water cause the solar radiation transmission maximum to shift towards longer wavelengths relative to those of clear oceanic water (Kowalczuk et al. 1999, Darecki et al. 2003, Kowalczuk et al. 2005). Estimating the quantitative and qualitative impact of CDOM absorption on AOP enabled a regional empirical algorithm to be constructed for estimating the CDOM absorption coefficient in the Baltic Sea (Kowalczuk et al. 2005). The aims of this study were i) to validate this algorithm and other existing algorithms embedded in the SeaDAS ocean colour imagery processing software over the Baltic Sea region, ii) to present examples of the application of the local empirical algorithm in the production of maps of $a_{\mathrm{CDOM}}(400)$ in the Baltic Sea, and iii) to present patterns of its seasonal spatial distribution.

2. Methods

2.1. In situ sampling of inherent and apparent optical properties

Field samples were collected between February 2000 and October 2008 as part of the Baltic Sea bio-optical observation programme carried out by the Institute of Oceanology at the Polish Academy of Sciences. Water samples for CDOM absorption were collected during 43 cruises in the southern Baltic Proper (Figure 1) covering the months from February to May and September to November. The geographical coverage of the samples includes the Gulf of Gdańsk, the Pomeranian Bay, Polish and German coastal waters, and the open sea (Baltic Proper). The coastal sites are under the direct influence of two major river systems (the Vistula and Oder), which drain the majority of Poland. Water samples were collected at fixed depths with Niskin bottles, the majority of samples being taken from the photic zone. Water samples for CDOM underwent a two-step filtration process. The first filtration was through acid-washed Whatman glass fibre filters (GF/F, nominal pore size

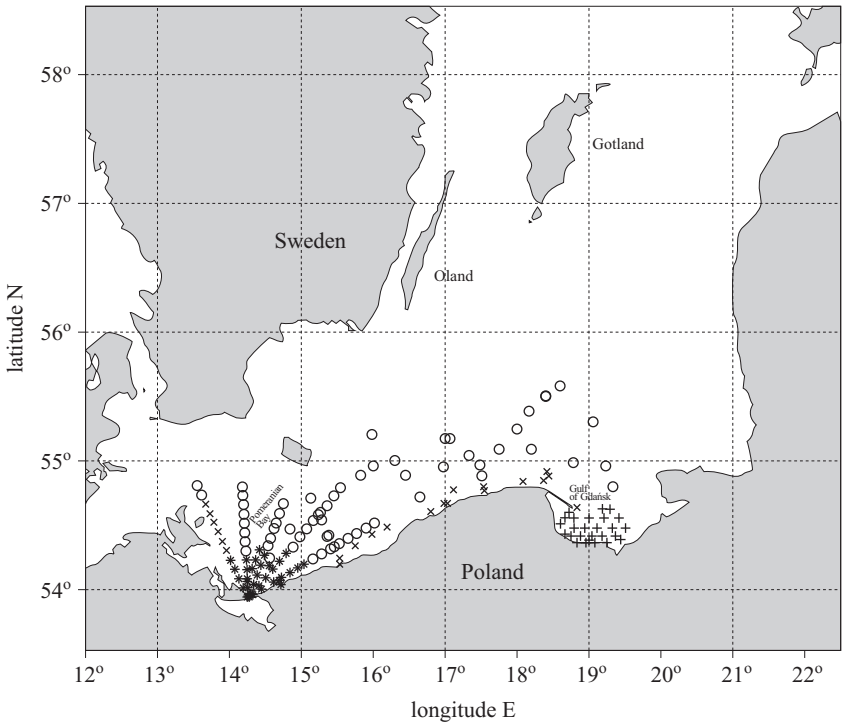

Figure 1. Grid of sampling stations used in the IO PAN remote sensing calibration-validation program: (+) sampling stations in the Gulf of Gdansk, (∗) sampling stations in the Pomeranian Bay, (∘) open sea sampling stations, (×) coastal zone sampling stations

0.7 μm). The water was then passed through Sartorius 0.2 μm pore cellulose membrane filters to remove fine-sized particles. Spectral absorption by CDOM was measured in the laboratory on board r/v 'Oceania' using a double-beam Unicam UV4-100 spectrophotometer with a 5-cm quartz cell in the 200–700 nm spectral range. MilliQ water was used as the reference for all measurements. The absorption coefficient $a_{\mathrm{CDOM}}(\lambda)$ was calculated using the following equation:

$$a_{\mathrm{CDOM}}(\lambda) = \frac{2.303A(\lambda)}{l}, \tag{2}$$

where $A(\lambda)$ is absorbance (optical density) and l is path length.

Measurements of the remote sensing reflectance and diffuse attenuation coefficient for downwelling irradiance were made using a MER2040 profiling spectroradiometer (Biospherical Instruments Inc., San Diego, USA). The instrument was equipped with 10 spectral channels (412, 443, 490, 510, 550, 565, 590, 625, 665, 710 nm) for both upwelling radiance (L_{u}) and downwelling irradiance (E_{d}) measurements. The radiometer was calibrated every one or two years at the manufacturer's laboratory. The dark current readings were monitored and the appropriate corrections were applied at all times. The measurement protocol was consistent with the reflectance measurements protocol for the SeaWiFS Project (Mueller & Austin 1992, 1995, Fargion & Mueller 2000) including correction for self-shading (Gordon & Ding 1992, Zibordi & Ferrari 1995). A MER 2040 spectroradiometer was deployed using a 6–8 m boom on the sunny side of the ship's stern to minimise the shading effect of the research vessel. The MER2040 measurements were accompanied by above-water measurements of spectral downwelling irradiance $E_{\mathrm{s}}(\lambda)$ with a sensor mounted on the ship's deck. All profiles of $E_{\mathrm{d}}(z, \lambda)$ and $L_{\mathrm{u}}(z, \lambda)$ and above-water measurements of $E_{\mathrm{s}}(\lambda)$ were plotted and examined carefully as a quality check. All measurements in which significant and rapid changes in the ambient light occurred during vertical profiling and those with any unusual spectra were eliminated from the analysis.

The remote-sensing reflectance $\mathrm{R_{rs}}(\lambda)$ was calculated as the ratio of the upwelling radiance just above the water surface $L_{\mathrm{w}}(\lambda)$ to the downwelling irradiance measured above the water $E_{\mathrm{s}}(\lambda)$. The water-leaving radiance $L_{\mathrm{w}}(\lambda)$ was obtained from the upwelling radiance estimated just below the water surface $L_{\mathrm{u}}(z = 0-, \lambda)$ and propagated through the water-air interface using a factor of 0.545 (assuming the refractive index of water relative to air to be ca 1.34). To obtain $L_{\mathrm{u}}(z = 0-, \lambda)$, the measurements of the upwelling radiance $L_{\mathrm{u}}(z, \lambda)$ were extrapolated from a depth of 1.5–2 m to the surface using the attenuation coefficient for upwelling radiance $K_{L_{\mathrm{u}}}(z, \lambda)$. $K_{L_{\mathrm{u}}}(z, \lambda)$ was calculated as the local slope of $\ln[L_{\mathrm{u}}(z, \lambda)]$ measured within

a depth interval spanning a few metres in the surface layer. The thickness of this depth interval depended on the extent to which the surface layer was homogeneous. Typically, it was about 3 metres. The noisy part of the data near the water surface (usually from 0 m to 0.3–0.7 m) was excluded from the calculation of $K_{L_u}(\lambda)$. In a similar way, the diffuse attenuation coefficient for downwelling irradiance $K_d(z, \lambda)$, used in the self-shading correction, was calculated from the $E_d(z, \lambda)$ profiles. The self-shading correction algorithm requires knowledge of the diffusivity of the natural light field over the sea surface. This parameter, defined as the ratio of the diffuse and direct incident solar irradiances, was measured with the shadow band radiometer developed at IO PAN (Olszewski et al. 1995), simultaneously with deployments of the profiling radiometers.

2.2. Satellite imagery and validation procedure

Ocean colour satellite imagery of the Baltic Sea from two scanners – SeaWiFS and MODIS Aqua – were acquired from the Goddard Space Flight Center, Distributed Active Archive Center, NASA. To provide sufficient validation data points, the time window between the satellite overpass and field sampling was set to ±8 hours, which represents the time windows for samples collected during the same day of the satellite overpass. Figure 2 shows the histogram of the time differences between the satellite overpass and the time of the in situ measurements. In situ measurements taken more than 5 hours before or after the satellite overpass made up only a small

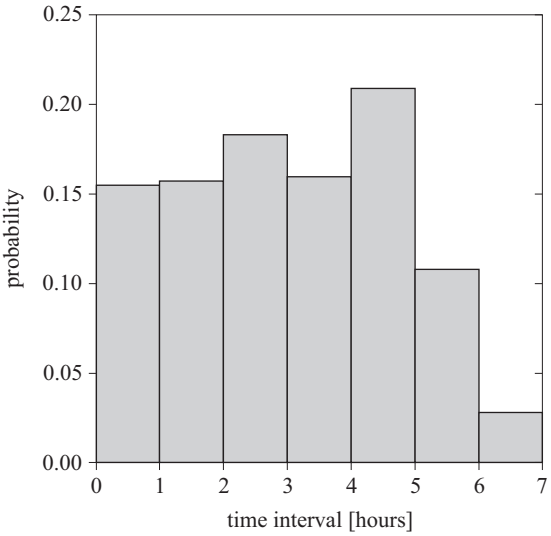

Figure 2. Histogram of the time differences between the satellite overpass and in situ measurements

proportion in our data set. Although Bailey & Werdell's (2006) procedure for validating the satellite ocean colour product requires the average value of the water-leaving radiance calculated from the 5x5 pixel box centred at the field station locations, the current study used the single pixel closest to the field sampling site owing to the high spatial heterogeneity of the optical properties of Baltic Sea waters. The patchiness effect described by Sagan (1991) can be found in the Baltic Sea not only in the coastal zone but also in the open water of the Baltic Proper. The spatial range of the observed inhomogeneities were from 0.3 to 3 km, and there was a maximum sixfold recorded difference in the magnitudes of the spectral values of the beam attenuation coefficient. 33 SeaWiFS 1 km resolution cloud-free and partially cloudy scenes between September 1997 and October 2004 were used in this analysis. A total number of 105 in situ IOP and AOP measurements and matching SeaWiFS pixels were used, as were 97 MODIS Aqua cloud-free or partly cloudy 1 km resolution scenes from March 2000 to October 2008. The total number of in situ IOP and AOP measurements and matching MODIS pixels was 134. The selected SeaWiFS and MODIS scenes were processed using SeaDAS software version 5.3. Darecki & Stramski (2004) demonstrated that the standard atmospheric correction used in the processing of SeaWiFS and MODIS ocean colour imagery is inadequate in the Baltic Sea and leads to very large errors in chlorophyll *a* and CDOM absorption estimates. Therefore, the MUMM atmospheric correction model was applied (Ruddick et al. 2000), which was designed to process ocean colour imagery in optically complex coastal and turbid waters, and is implemented in SeaDAS software given by standard SeaDAS atmospheric correction. The MUMM atmospheric correction significantly reduces the number of pixels with negative water-leaving radiance values in the 412 and 443 nm spectral bands (Moses et al. 2009). The atmospherically corrected spectral values of normalised water-leaving radiances of pixels that matched the location of in situ measurements were extracted from processed scenes and imported into Excel spreadsheets. The spectral values of normalised water-leaving radiances were then converted into remote sensing reflectance values by dividing them by the mean extraterrestrial solar irradiance $F_0(\lambda)$, corresponding to the SeaWiFS/MODIS spectral band. The spectral reflectances were further used to calculate the CDOM absorption coefficient $a_{\mathrm{CDOM}}(400)$ using the Kowalczuk et al. (2005) algorithm

$$a_{\mathrm{CDOM}}(400) = 10^{(-0.29-0.708\,X+1.12\,X^2)}, \tag{3}$$

where $X = \log 10(\mathrm{R_{rs}}(490)/\mathrm{R_{rs}}(555))$.

Additionally, two semi-analytical algorithms implemented in the SeaDAS processing software were used – the GSM-01 algorithm (Garver & Siegel

1997) and the Carder 99 algorithm (Carder et al. 1999) – to produce CDOM absorption coefficients at 412 nm – $a_{\mathrm{CDOM}}(412)$. These values were also used to test their applicability in the Baltic Sea region.

The best examples of processed MODIS Aqua scenes presenting a cloud-free view of the Baltic Sea were used to produce $a_{\mathrm{CDOM}}(400)$ maps to illustrate its spatial distribution in the study area in different seasons.

3. Results

3.1. Validation of the CDOM absorption coefficient product from the Kowalczuk et al. (2005) empirical algorithm in the Baltic Sea

The assessment of algorithm performance was based on the statistical parameters of comparing the satellite-derived retrievals of $a_{\mathrm{CDOM}}(400)$ and $a_{\mathrm{CDOM}}(412)$ with field measurements, which are referred to here as validation match-ups. The statistical parameters applied include the percentage difference (PD) defined by equation (4); *Bias* defined by equation (5); root mean square error (RMSE) defined by equation (6); and the coefficient of determination R^2 and the slopes and intercepts of the linear regression between the satellite algorithm estimates and in situ measurements on the log-log scale (Bailey & Werdell 2006, Melin & Maritorena 2007). In the following equations, X_{sat} and $X_{\mathrm{in\,situ}}$ represent the parameters of interest ($a_{\mathrm{CDOM}}(400)$ or $a_{\mathrm{CDOM}}(412)$) for the satellite algorithm and field observations respectively, and N refers to the sample size.

$$\mathrm{PD} = \frac{X_{\mathrm{sat}} - X_{\mathrm{in\,situ}}}{X_{\mathrm{in\,situ}}} \times 100\%, \tag{4}$$

$$Bias = \frac{1}{N}\sum_{i=1}^{N}(X_{\mathrm{sat}} - X_{\mathrm{in\,situ}}), \tag{5}$$

$$\mathrm{RMSE} = \sqrt{\frac{1}{N}\sum_{i=1}^{N}(X_{\mathrm{sat}} - X_{\mathrm{in\,situ}})^2}. \tag{6}$$

The Kowalczuk et al. (2005) empirical band ratio algorithm for estimating the CDOM absorption coefficient $a_{\mathrm{CDOM}}(400)$ was constructed from a set of 577 simultaneous radiometric and in situ IOP measurements collected between 1993 and 2000. In the first step of the validation analysis, we wanted to test this algorithm using an independent set of IOP and AOP measurements. Although the data set volume of optical measurements conducted in the Baltic Sea after 2000 was comparable with the data set

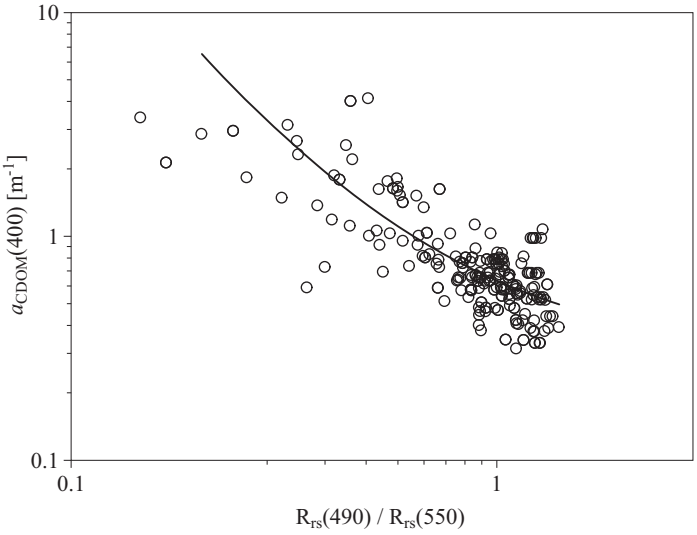

Figure 3. Distribution of $a_{\mathrm{CDOM}}(400)$ as a function of the spectral reflectance band ratio $\mathrm{R_{rs}}(490)/\mathrm{R_{rs}}(550)$ measured in situ. Data collected between 2000 and 2008. The solid line represents the empirical relationship between $a_{\mathrm{CDOM}}(400)$ and log transformed $\mathrm{R_{rs}}(490)/\mathrm{R_{rs}}(550)$ derived by Kowalczuk et al. (2005)

used for algorithm construction, we only used 257 radiometric and IOP samples that were coincident with the cloud-free or partly cloudy SeaWiFS and MODIS scenes used in this study. Figure 3 presents the distribution of $a_{\mathrm{CDOM}}(400)$ values as a function of the $\mathrm{R_{rs}}(490)$ and $\mathrm{R_{rs}}(550)$ band ratios in the data set used for this validation study. On top of the scatter plot we have overlain the second-order polynomial function representing the empirical algorithm derived by Kowalczuk et al. (2005). The overlain function fits the distribution of the validation data set quite well, with the exception of a few points at high CDOM absorption values. The range of variability of the CDOM absorption coefficient $a_{\mathrm{CDOM}}(400)$ in the data set selected for this study is from 0.12 to 5.4 m^{-1}, which is within the published range of variability of the CDOM absorption coefficient in the Baltic Sea (Kowalczuk 1999, Kowalczuk et al. 2006). This small data set therefore provides a good representation of the CDOM absorption conditions in the study area.

The comparison of the CDOM absorption coefficient values derived from equation (3) with those measured in situ is presented in Figure 4 (left-hand panel). The distribution of the percentage differences between the satellite algorithm estimates and the in situ measurements is shown in the right-hand panel of Figure 4. The matching points are quite uniformly distributed around the 1:1 line, without distinct trends of either under- or overestimation. The range of variability in the percentage differences

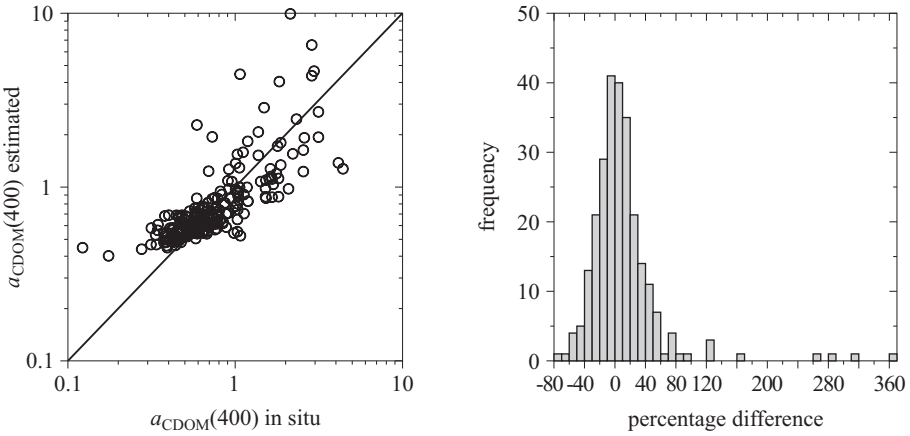

Figure 4. Relationship between the CDOM absorption coefficient $a_{\mathrm{CDOM}}(400)$ measured in situ in the Baltic and that estimated with the Kowalczuk et al. (2005) algorithm (left-hand panel) and the histogram (right-hand panel) of the percentage error in the estimate of the CDOM absorption coefficient $a_{\mathrm{CDOM}}(400)$ using equation (3) with the in situ reflectance data set

was from -71.09% to 364.68%. The smallest PD between the satellite algorithm estimate based on in-water radiometric measurements and the true $a_{\mathrm{CDOM}}(400)$ value measured in the sea water was -0.07%. The satellite algorithm tested using the independent in-water radiometric values have quite a small systematic error, the calculated value of which was $Bias = 0.05$. However, there was considerable dispersion of the matching points. The mean square root error, which is a measure of dispersion, was $\mathrm{RMSE} = 0.75$. The slopes and intercepts of the linear regression between satellite algorithm estimates and the in situ $a_{\mathrm{CDOM}}(400)$ values on a log-log scale were $a = 0.69$ and $b = -0.07$ respectively, and the coefficient of determination was $\mathrm{R}^2 = 0.59$.

The majority of points on the histogram of the percentage error of estimation shown in Figure 4 is equally distributed around 0, and the distribution is close to normal. However, the tail of points located on the far right of the histogram departs significantly from the general distribution; it presumably belongs to a different population. The geographical location of these points and the time difference between the in situ measurements and satellite overpasses were examined in detail. It appears that all but one of the points are located in the Gulf of Gdańsk in close proximity to the Vistula River mouth. The river discharges fresh water containing high loads of CDOM and suspended material, and riverine plumes are readily identified in sea water by their optical properties. The mixing of fresh and saline water is intensified by coastal currents and waves. Sagan (2008) measured very

high rates of dynamic changes in the optical properties of sea water in this region on a temporal scale of minutes and a spatial scale of tens of metres. As a result of the mixing, the water has a patchy structure, and lenses of water with distinctly different physical and optical properties are contiguous. Although the AOP and IOP optical measurements and water sampling for IOP on board r/v 'Oceania' were conducted quasi-simultaneously (the time difference between each cast and water sampling was reduced to a minimum) and multiple optical sensors were deployed simultaneously, the lowering winches were separated by a distance of ca 15 m to stop the instruments from getting tangled up. But even these precautions did not prevent distinctly different patches of water from being sampled. Sagan (2008) gives examples of absorption and scattering coefficients derived from the measurement of two AC-9 casts made at 5 minute intervals, which were used to produce the spectral values of the absorption and backscattering coefficients according to the spectral dependency between the $b(\lambda)/b_{\mathrm{b}}(\lambda)$ ratio (Aas et al. 2005) and the averaged values of $b_{\mathrm{b}}(\lambda)$ in the Baltic Sea water taken from Siegel et al. (2005). Model-derived coefficients were used to produce the spectral reflectance spectra according to the classic Morel & Gentili (1993) formulae, and these in turn were used in the O'Reilly OC4v4 algorithm (1998) to obtain the chlorophyll *a* concentrations. Those two measurements of inherent optical properties taken at 5 minute intervals resulted in a 60% difference in the chlorophyll *a* concentration product. Therefore, it is likely that the natural physical phenomena in the vicinity of the Vistula River mouth which drive the very high variability of optical properties and create water patchiness are the main sources of such large differences between in situ measurements and algorithm estimates.

Only 22 samples diverge from the populations of the normal distribution of percentage error of estimates (error greater than ±80%), which corresponds to just 8.5% of the samples used in the validation study. In the current study, these are considered to be outliers, and were excluded from further analysis. Excluding the outliers significantly improves the comparison of the in situ measurements and the Kowalczuk et al. (2005) algorithm estimates of $a_{\mathrm{CDOM}}(400)$ values: the percentage error of estimates was reduced to a narrower range, from −71.09% to 79.55%. The smallest PD between the satellite algorithm estimate based on in-water radiometric measurements and the true $a_{\mathrm{CDOM}}(400)$ value measured in sea water was −0.07%. *Bias* and RMSE were much smaller at $Bias = -0.02$, $\mathrm{RMSE} = 0.46$; and the coefficient of determination was significantly greater $\mathrm{R}^2 = 0.70$. Figure 5 (left-hand panel) presents the distribution of the values of $a_{\mathrm{CDOM}}(400)$ measured in situ versus the algorithm estimates. The much smaller scatter over the 1:1 line is noticeable, and the histogram of

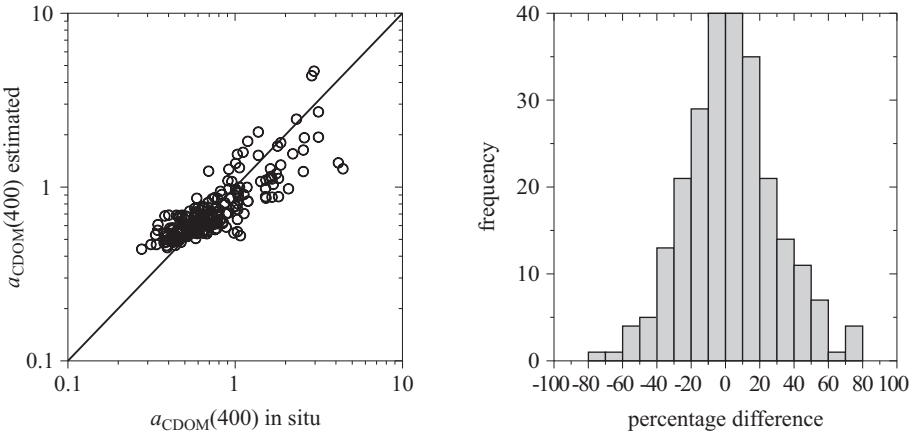

Figure 5. Relationship between the CDOM absorption coefficient $a_{\mathrm{CDOM}}(400)$ measured in situ in the Baltic and that estimated with the Kowalczuk et al. (2005) algorithm (left-hand panel) and the histogram (right-hand panel) of the percentage error in the estimate of the CDOM absorption coefficient $a_{\mathrm{CDOM}}(400)$ using equation (3) with the in situ reflectance data set after eliminating outliers

the percentage error of estimates shown has a nearly normal distribution, without any outlying points (see Figure 5, right-hand panel).

In the second stage of the analysis, the remote sensing reflectance derived from SeaWiFS and MODIS ocean colour imagery was applied after atmospheric correction with the MUMM model. The validation results are

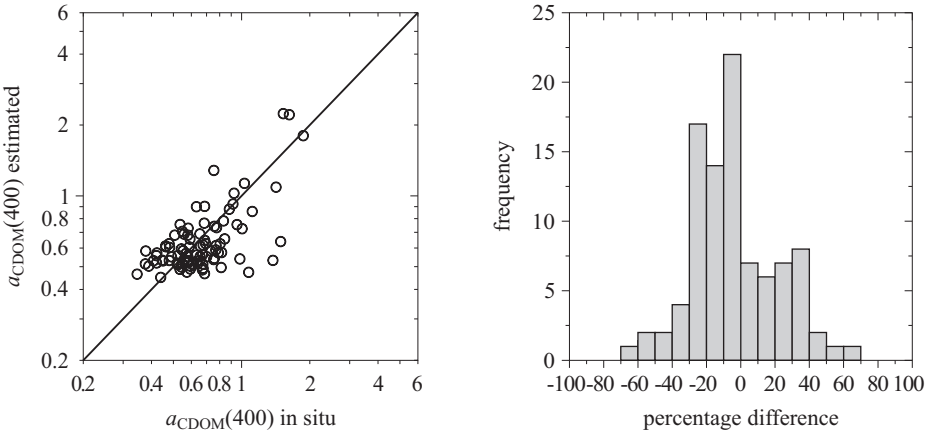

Figure 6. Relationship between the CDOM absorption coefficient $a_{\mathrm{CDOM}}(400)$ measured in situ in the Baltic and that estimated with the Kowalczuk et al. (2005) algorithm (left-hand panel) and the histogram (right-hand panel) of the percentage error in the estimate of the CDOM absorption coefficient $a_{\mathrm{CDOM}}(400)$ using equation (3) with the SeaWiFS reflectance data set

satisfactory although the calculated statistics, the distribution of points on the 1:1 line, and the distribution of the percentage error of the estimates on the histogram suggest an overall deterioration of algorithm performance in comparison to the Kowalczuk et al. (2005) algorithm product using the in situ remote sensing reflectance data set. Figure 6 shows the distribution of match-up points over the 1:1 line and the histogram of distribution of the percentage error of the estimates of $a_{\mathrm{CDOM}}(400)$ values using the Kowalczuk et al. (2005) algorithm with the SeaWiFS remote sensing reflectance data set. Figure 7 shows the results of a similar analysis, but with the MODIS remote sensing reflectances applied to equation (3). The data sets presented in the figures do not contain samples identified as outliers. Table 1 presents detailed results of the statistical analysis. The statistical metrics calculated for the differences between the data are better for SeaWiFS than those for the MODIS data set; e.g. the coefficient of determination for the SeaWiFS data set was $\mathrm{R}^2 = 0.40$ versus $\mathrm{R}^2 = 0.29$ for the MODIS data.

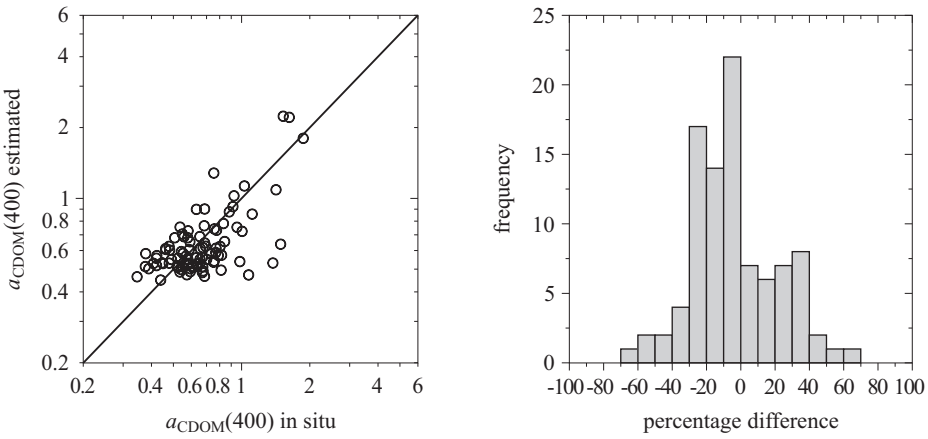

Figure 7. Relationship between the CDOM absorption coefficient $a_{\mathrm{CDOM}}(400)$ measured in situ in the Baltic and estimated with the Kowalczuk et al. (2005) algorithm (left-hand panel) and the histogram (right-hand panel) of the percentage error in the estimate of the CDOM absorption coefficient $a_{\mathrm{CDOM}}(400)$ using equation (3) with the MODIS Aqua reflectance data set

3.2. Validation of the CDOM absorption coefficient product from the Carder-99 and GSM-01 semi-analytical algorithms in the Baltic Sea

The SeaDAS version 5.3 processing software includes two semi-analytical algorithms – GSM_01 (Garver & Siegel 1997) and Carder-99 (Carder et al. 1999) – which produce CDOM absorption coefficient values for 412 nm.

Table 1. Detailed results of the statistical analysis of CDOM absorption product validation derived from different algorithms with in situ spectral reflectance and SeaWiFS and MODIS ocean colour imagery data between 2000 and 2006

	PD range [%]	Smallest PD [%]	*Bias*	RMSE	R^2	Slope	Intercept	*N*
Kowalczuk et al. (2005) R_{rs} in situ, all data	−71.09 – 364.68	0.07	0.05	0.75	0.59	0.69	−0.07	257
Kowalczuk et al. (2005) R_{rs} in situ, without outliers	−71.09 – 79.55	0.07	−0.02	0.46	0.70	0.63	−0.13	235
Kowalczuk et al. (2005) R_{rs} SeaWiFS, without outliers	−61.36 – 69.81	−0.69	−0.02	0.23	0.40	0.58	−0.22	94
Kowalczuk et al. (2005) R_{rs} MODIS, without outliers	−53.79 – 76.32	0.75	−0.03	0.19	0.29	0.38	−0.37	122
Carder MODIS	−96.30 – 67.66	1.17	−0.40	0.63	0.02	0.22	−1.80	135
Carder SeaWiFS	−97.38 – 56.76	−6.63	−0.44	0.66	0.01	0.14	−1.80	76
GSM_01 MODIS	−96.42 – 1108.65	5.11	−0.15	0.75	0.01	0.09	−1.62	117
GSM_01 SeaWiFS	−97.81 – 293.73	−4.10	−0.29	0.66	0.09	0.51	−1.21	80

The performance of these two algorithms was tested in the Baltic Sea. The overall results of validation demonstrated that both semi-analytical algorithms significantly and systematically underestimate the CDOM absorption coefficient. The statistical metrics calculated for the Carder-99 algorithm for both the SeaWiFS and MODIS data sets returned high negative *Bias* and high RMSE values (see Table 1). The statistical metrics calculated for the GSM_01 algorithm returned smaller *Bias* and higher RMSE than did the Carder-99 algorithm. The percentage error of estimates was largest when the GSM-01 algorithm was applied to MODIS data.

3.3. The application of the Kowalczuk et al. (2005) algorithm for mapping the CDOM absorption coefficient $a_{\mathrm{CDOM}}(400)$ in the Baltic Sea: some examples

Thirty-six cloud-free MODIS scenes of the Baltic Sea were selected to explore the utility of ocean colour imagery for mapping the spatial distribution of the CDOM absorption coefficient, $a_{\mathrm{CDOM}}(400)$. The scenes cover the period between 2004 and 2008, but they are unevenly distributed seasonally. Cloud cover prevented the collection of cloud-free scenes in the autumn, and there are no cloud-free scenes coinciding with in situ measurements after September in any year examined in this study. Therefore, the scenes presented in Figure 8 show the $a_{\mathrm{CDOM}}(400)$ spatial distribution patterns typical of winter conditions before the phytoplankton bloom starts, during the spring bloom, and also during a cyanobacteria bloom in the summer and after its collapse in early autumn.

The seasonal distribution of the CDOM absorption coefficient follows the pattern that was reported previously on the basis of in situ measurements. The CDOM absorption level increases during spring and summer, and then decreases to its minimum in winter (Kowalczuk 1999). The synoptic view of satellite sensors reveals the spatial pattern of $a_{\mathrm{CDOM}}(400)$ distribution. Vast areas of the Baltic Sea are almost homogeneous in terms of CDOM absorption in winter, except in the coastal zone, where there is a belt of water close to the shore with elevated CDOM absorption values. There are conspicuous areas of riverine plume discharge, where $a_{\mathrm{CDOM}}(400)$ values are significantly higher. These areas clearly mark the dispersion range of riverine waters; for example, the Vistula river plume is clearly visible in the Gulf of Gdańsk, extending to the open water north of Cape Rozewie. Smaller plumes are visible in the Pomeranian Bay near the Świna River mouth and near Klaipeda, where an inlet connects the Curonian Lagoon with coastal waters.

Satellite imagery indicates that phytoplankton blooms in spring and late summer can be an important source of CDOM in the Baltic Sea.

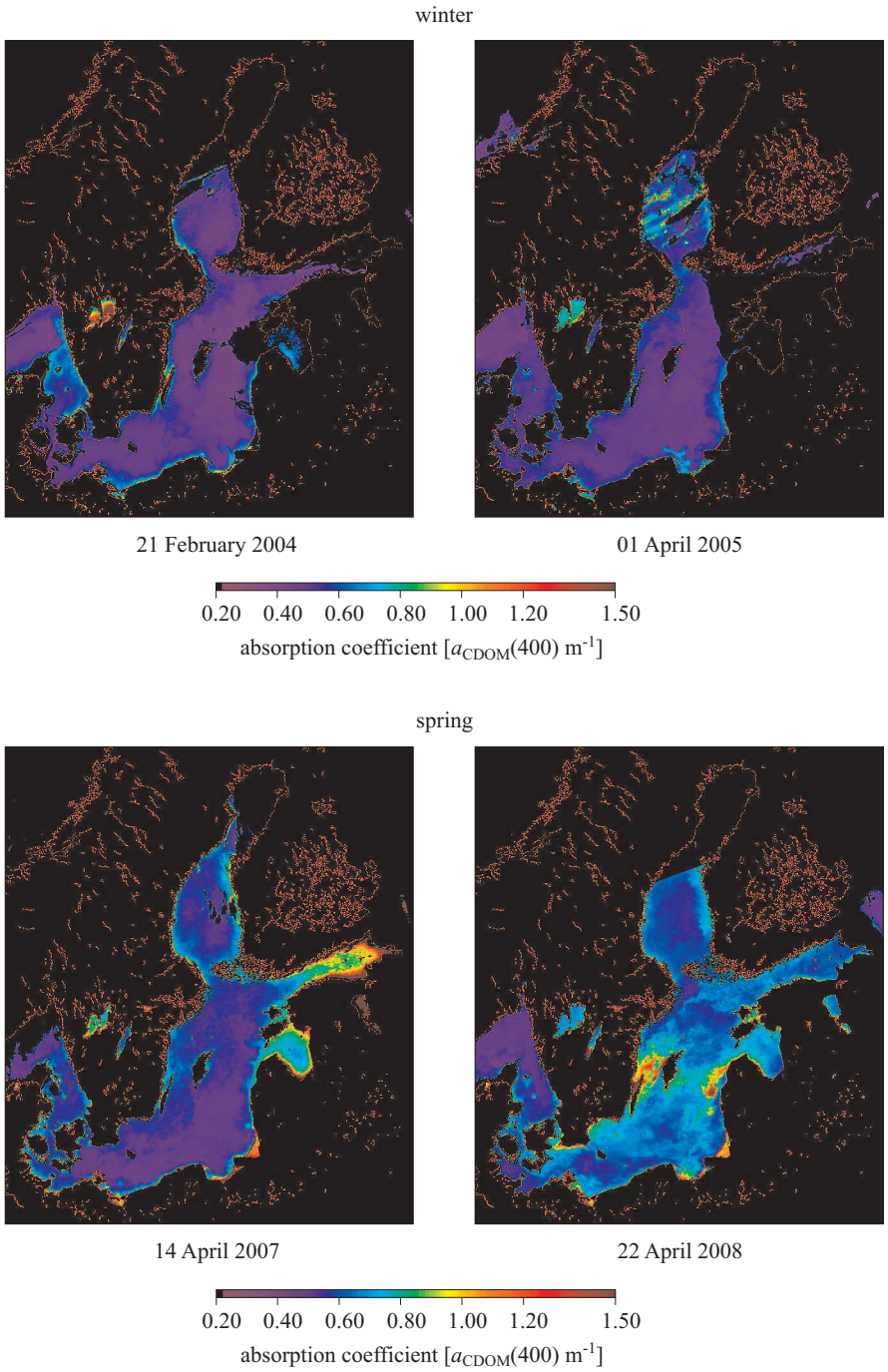

Figure 8. Maps of the CDOM absorption coefficient $a_{\mathrm{CDOM}}(400)$ in the Baltic Sea produced by applying the Kowalczuk et al. (2005) algorithm to MODIS data in different seasons: some examples (*continued on next page*)

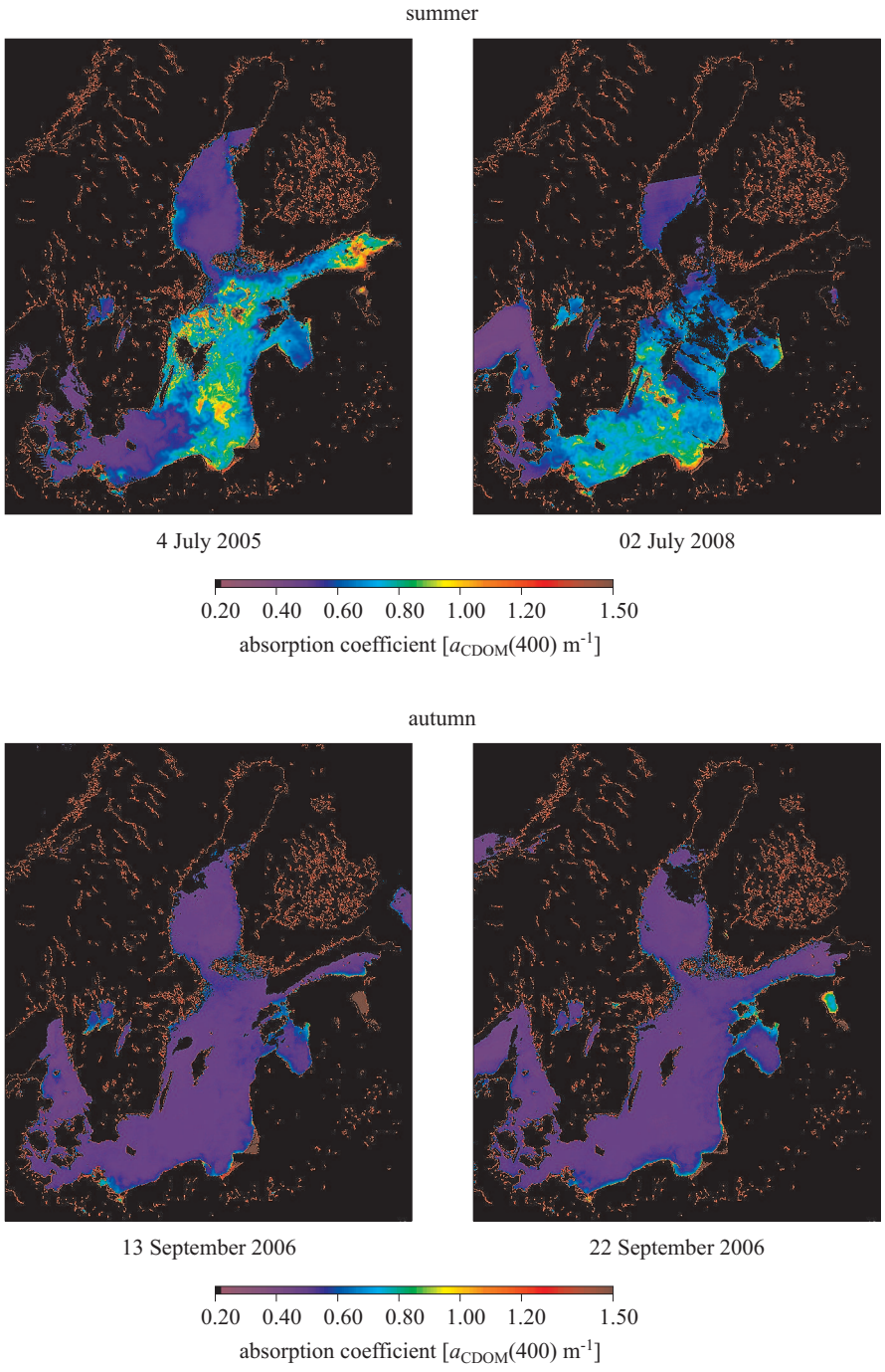

Figure 8. (*continued*)

The first spring scene, acquired on 14 April 2007, depicts the pre-bloom situations with elevated CDOM absorption coefficient $a_{\mathrm{CDOM}}(400)$ values in the Gulf of Riga, Gulf of Gdańsk and Pomeranian Bay, which are related to the annual maximum river flow from the Baltic Sea catchment area. Another scene from April presents the spatial distribution of $a_{\mathrm{CDOM}}(400)$ during an extensive phytoplankton bloom in the Baltic Proper, the Gulf of Gdańsk, and between the east coast of Sweden and Gotland. The $a_{\mathrm{CDOM}}(400)$ distribution pattern is very similar to the spatial features on the maps of chlorophyll *a* concentration produced from SeaWiFS and MODIS imagery during blooms (Kahru 1997, Kutser 2004, Reinart & Kutser 2006, Kahru et al. 2007). The last two examples (scenes acquired on 13 and 22 September 2006) of $a_{\mathrm{CDOM}}(400)$ present the situation after the cessation of biological activity in autumn; the particulate and dissolved material accumulated in the surface waters quickly disperses in the water column and the $a_{\mathrm{CDOM}}(400)$ spatial distribution is close to that observed in winter.

4. Discussion and summary

The aim of the SeaWiFS mission was to achieve an overall accuracy of 35% in estimating chlorophyll *a* concentrations in oceanic waters (Hooker & Esaias 1993). The mission was accomplished, as the global validation study by Gregg & Casey (2004) of over 4000 in situ and satellite estimate match-ups indicated that the average estimation error of chlorophyll *a* concentrations using the O'Reilly OC4v4 algorithm was RMSE = 0.31 with $\mathrm{R}^2 = 0.76$. However, Gregg & Casey pointed out that, if samples from coastal oceans, high latitudes and semi-enclosed seas were excluded, the overall accuracy of the algorithm would be better than 30%. One of the regions with the poorest validation results was the Baltic Sea at RMSE = 0.494 and $\mathrm{R}^2 = 0.02$. A detailed validation study of the SeaWiFS and MODIS products in the Baltic Sea region by Darecki & Stramski (2004) identified serious problems with using ocean colour imagery in this region: the application of standard retrieval algorithms and standard atmospheric corrections would lead to estimation errors of up to 200%. Darecki & Stramski tested a modified Carder-99 algorithm on in situ radiometric data. Retrievals of chlorophyll *a* values were quite good at $Bias = 0.04$ and RMSE = 0.30. They also tested the retrieval of $a_{\mathrm{CDOM}}(400)$ values from a modified Carder-99 algorithm, and the comparison of in situ values and estimates was quite good at $Bias = -0.07$ a RMSE = 0.40. The CDOM absorption coefficient $a_{\mathrm{CDOM}}(400)$ values calculated with the same algorithm but using MODIS radiometric quantities were much less accurate at $Bias = -0.69$ and RMSE = 0.21. However, these results were distorted by the very small sample size, only 9 matching points being selected.

To date, only a few algorithms specifically designed to estimate the CDOM absorption coefficient have been published. Most of the empirical band ratio algorithms use linear or non-linear combinations of SeaWiFS/MODIS wavebands (see Kahru & Mitchell 1999). Kahru & Mitchell (2001) used the power law approximation $R_{rs}(443)/R_{rs}(510)$ ratio to estimate CDOM absorption coefficients at 300 nm, and D'Sa & Miller (2003) presented a relationship of $a_{CDOM}(412)$ as a function of the log transformed ratio of $R_{rs}(510)/R_{rs}(555)$. Mannino et al. (2008) used exponential and linear approximations of different log transformed band ratios of $R_{rs}(412)/R_{rs}(555)$, $R_{rs}(490)/R_{rs}(555)$ and $R_{rs}(510)/R_{rs}(555)$ to estimate $a_{CDOM}(355)$. Spectral bands of satellite sensors situated in the blue part of the light spectrum are useless in optically complex coastal waters, where there is a high CDOM concentration. The level of upwelling radiance in the 412 nm or 443 nm spectral bands is very small (e.g. Kowalczuk et al. 2005). As CDOM absorption increases, the spectral reflectance band ratio uses reflectance values at wavelengths longer than 443 nm in the numerator and $R_{rs}(555)$ in the denominator. Kowalczuk et al. (2005) have shown that the $R_{rs}(490)/R_{rs}(590)$ band ratio algorithm was much more accurate in estimating $a_{CDOM}(400)$ in the Baltic Sea than the $R_{rs}(490)/R_{rs}(555)$ band ratio algorithm. Unfortunately, the 590 nm spectral band is currently unavailable in operational ocean colour satellite sensors. Recently, Kutser et al. (2009) developed an empirical band ratio algorithm for estimating CDOM absorption from ocean colour satellite imagery in Estonian coastal waters using a power function of the spectral reflectance ratio of two bands of the Advanced Land Imager (Band 4: 525–605 nm, and Band 5: 630–690 nm). The accuracies of published algorithms for the retrieval of CDOM absorption coefficient values are as follows: Kahru & Mitchell (2001) RMSE = 0.197, $R^2 = 0.80$, $N = 11$; the Carder et al. (1999) semi-analytical algorithm RMSE = 0.405, $R^2 = 0.751$, $N = 26$; Mannino et al. (2008) RMSE = 0.25, $R^2 = 0.68$, $N = 49$.

The validation results of the empirical band ratio algorithm by Kowalczuk et al. (2005) presented in the current study is satisfactory. It is difficult to perform calibration-validation studies in the Baltic Sea area because of the extensive cloud cover there, the low number of cloud-free days, the low levels of incident solar radiation in the winter months reducing the $L_{nw}(\lambda)$ signal below the detection threshold, and the optical complexity of the waters. The problems of the lack of a proper atmospheric correction model for a high-latitude, semi-enclosed sea, and the complexity of the optical properties of Baltic Sea waters remain unresolved. All these factors in combination with the very high spatial and temporal variability of optical properties on the sub-pixel scale, especially in coastal areas, make

direct comparisons of in situ values and satellite algorithm products very difficult. At best, CDOM absorption coefficient values of $a_{\mathrm{CDOM}}(400)$ can be estimated with an average accuracy of 23%. It should be emphasised that the algorithms were not validated in coastal areas, but it is likely that the error of the estimates of $a_{\mathrm{CDOM}}(400)$ values will be substantial (in excess of 100%). It should also be noted that existing operational semi-analytical retrieval algorithms for IOP generally fail in the Baltic Sea, and that both the tested algorithms underestimate the CDOM absorption coefficient substantially.

The examples of the spatial distribution of the CDOM absorption coefficient $a_{\mathrm{CDOM}}(400)$ presented in this study correspond well with general knowledge of the spatial and temporal distribution of this parameter gained through field studies and in situ sampling and reported in the papers by Kowalczuk (1999) and Kowalczuk et al. (1999, 2005). The overall trend in seasonal changes shown on the satellite scenes indicates that there is an increase in the absorption level in spring, first in the bays close to riverine input, then in open waters. This is later followed by a slow decrease to the winter minimum of CDOM absorption. Compared to our results with published satellite imagery showing the distribution of chlorophyll *a* in the surface water of the Baltic Sea (Kahru et al. 2007), we found by analogy a similarity in the spatial distribution between $a_{\mathrm{CDOM}}(400)$ and chlorophyll *a* concentration, especially during the fully-developed spring phytoplankton bloom and the summer cyanobacteria bloom. Modelling studies based on in situ measurements have demonstrated that chlorophyll *a* is an important factor determining the CDOM absorption coefficient in spring and summer, especially at salinities higher than 7.00 and in areas beyond the direct influence of riverine discharge (Kowalczuk et al. 2006). Siegel et al. (2005a) reassessed the bio-optical assumption based on inherent optical properties ($a_{\mathrm{ph}}(443)$, $a_{\mathrm{CDM}}(443)$ and $b_{\mathrm{bp}}(443)$) and chlorophyll *a* concentrations derived from the semi-analytical GSM_01 model applied to a global data base of SeaWiFS scenes and the analysis of common forcing mechanisms that control the variability of optical properties and phytoplankton biomass. They found that, in most cases, CDOM and phytoplankton pigment absorption is correlated on a global scale, especially at high latitudes (40 degrees and higher) in the northern hemisphere. Seasonal and inter-annual changes in both parameters in these regions of the global ocean are also closely coupled. Siegel et al. (2005b) state that CDOM absorption and chlorophyll *a* concentrations could be uncoupled in coastal zones of oceans, and also in marginal and semi-enclosed seas such as the Baltic. The similarities in spatial and temporal distribution between $a_{\mathrm{CDOM}}(400)$ and chlorophyll *a* concentration in the Baltic Sea

may be driven by the coincidence of forcing factors: the maximum riverine outflow and the spring phytoplankton bloom occur at the same time in April. The annual warm-up melts the snow cover and the high radiation doses absorbed by the sea enable the formation of the thermocline and the fulfilment of Sverdrup's critical depth hypothesis (Sverdrup 1953), which triggers the phytoplankton bloom. During cyanobacteria blooms in summer, the organic matter, produced by filamentous organisms, that is released into the water accumulates in the shallow mixing zone together with phytoplankton cells. The spatial patterns therefore appear to be very similar on CDOM absorption coefficient and chlorophyll *a* concentration maps. The correlation between $a_{\mathrm{CDOM}}(400)$ and chlorophyll *a* concentrations should be confirmed by in situ measurements. There is a data record in our archive that indicates an increase of $a_{\mathrm{CDOM}}(400)$ in the Gdansk Deep, which is distant from riverine sources of terrestrial DOM, at the end of summer in August 1994 (Kowalczuk & Kaczmarek 1996). Since 1994, CDOM absorption measurements have never again produced such high values of $a_{\mathrm{CDOM}}(400)$. There is an urgent need to measure inherent and apparent optical properties during cyanobacteria blooms and to establish the relationships between $a_{\mathrm{CDOM}}(400)$ and chlorophyll *a* concentrations under these extreme conditions. One possible solution is to install CDOM fluorometers on existing and future FerryBox systems operating on ferries in the Baltic Sea.

Another source of the similarities between the spatial and temporal distributions of $a_{\mathrm{CDOM}}(400)$ and chlorophyll *a* concentrations could be the insufficient sensitivity of empirical algorithms for retrieving CDOM absorption and chlorophyll *a* concentrations. Both of the algorithms presented in the current paper use remote sensing reflectance in the same spectral band of 490 and 555 nm. The only difference between the algorithms is the fitting functional formulae used to regress the sensed parameter and the reflectance ratio in these two spectral bands. The sensitivity of empirical algorithms needs to be tested against the simulated remote sensing reflectance constructed with a known set of inherent and apparent optical properties. Such simulated spectral remote sensing reflectance, where the IOP are set as independent variables, should be used in algorithm sensitivity tests.

References

Aas E., Høkedal J., Sørensen K., 2005, *Spectral backscattering coefficient in coastal water*, Int. J. Remote Sens., 26 (2), 331–343.

Bailey S. W., Werdell P. J., 2006, *A multi-sensor approach for the on-orbit validation of ocean color satellite data products*, Remote Sens. Environ., 102 (1–2), 12–23.

Bélanger S., Xie H., Krotkov N., Larouche P., Vincent W. F., Babin M., 2006, *Photomineralization of terrigenous dissolved organic matter in Arctic coastal waters from 1979 to 2003: Interannual variability and implications of climate change*, Global Biogeochem. Cy., 20 (4), GB4005, doi:10.1029/2006GB002708.

Blough N. V., Del Vecchio R., 2002, *Chromophoric DOM in the coastal environment*, [in:] *Biogeochemistry of marine dissolved organic matter*, D. Hansell & C. Carlson (eds.),. Acad. Press, New York, 509–546.

Carder K. L., Chen F. R., Lee Z. P., Hawes S. K., 1999, *Semianalytic moderate-resolution imaging spectrometer algorithms for chlorophyll a and absorption with bio-optical domains based on nitrate-depletion temperatures*, J. Geophys. Res., 104 (C3), 5403–5421.

Darecki M., Stramski D., 2004, *An evaluation of MODIS and SeaWiFS bio-optical algorithms in the Baltic Sea*, Remote Sens. Environ., 89 (3), 326–350.

Darecki M., Weeks A., Sagan S., Kowalczuk P., Kaczmarek S., 2003, *Optical characteristics of two contrasting case 2 waters and their influence on remote sensing algorithms*, Cont. Shelf Res., 23, 237–250.

Del Castillo C. E., Miller R. L., 2008, *On the use of ocean color remote sensing to measure the transport of dissolved organic carbon by the Mississippi River Plume*, Remote Sens. Environ., 112 (3), 836–844.

Del Vecchio R., Subramaniam A., Uz S. Schollaert, Ballabrera-Poy R., Brown C. W., Blough N. V., 2009, *Decadal time-series of SeaWiFS retrieved CDOM absorption and estimated CO_2 photoproduction on the continental shelf of the eastern United States*, Geophys. Res. Lett., 36, L02602, doi:10.1029/2008GL036169.

D'Sa E. J., Hu C., Muller-Karger F. E., Carder K. L., 2002, *Estimation of colored dissolved organic matter and salinity fields in case 2 waters using SeaWiFS: Examples from Florida Bay and Florida Shelf*, Proc. Indian Acad. Sci. (Earth and Planetary Sciences), 111 (3), 197–207.

D'Sa E. J., Miller R. L., 2003, *Bio-optical properties in waters influenced by the Mississippi River during low flow conditions*, Remote Sens. Environ., 84 (4), 538–549.

Fargion G. S., Mueller J. L., 2000, *Ocean optics protocols for satellite ocean color sensor validation, Revision 2*, NASA Tech. Memo. 200-209966, NASA Goddard Space Flight Center, Greenbelt, MD.

Fichot C. G., Sathyendranath S., Miller W. L., 2008, *SeaUV and SeaUV(C): Algorithms for the retrieval of UV/visible diffuse attenuation coefficients from ocean color*, Remote Sens. Environ., 112 (4), 1584–1602.

Garver S. A., Siegel D. A., 1997, *Inherent optical property inversion of ocean color spectra and its biogeochemical interpretation, 1. Time series from the Sargasso Sea*, J. Geophys. Res., 102 (8), 18607–18625.

Gordon H. R., Ding K., 1992, *Self-shading of in-water instruments*, Limnol. Oceanogr., 37 (3), 491–500.

Gregg W. W., Casey N. W., 2004, *Global and regional evaluation of the SeaWiFS chlorophyll data set*, Remote Sens. Environ., 93 (4), 463–479.

Hansell D. A., Carlson C. A., 2001, *Marine dissolved organic matter and the carbon cycle*, Oceanography, 14 (4), 41–49.

Hooker S. B., Esaias W. E., 1993, *An overview of the SeaWiFS project*, Eos Trans. Amer. Geophys. Union, 74, 241–246.

Jerlov N. G., 1976, *Marine optics*, Elsevier, New York, 231 pp.

Johannessen S. C., Miller W. L., 2001, *Quantum yield for the photochemical production of dissolved inorganic carbon in seawater*, Mar. Chem., 76 (4), 271–283.

Johannessen S. C., Miller W. L., Cullen J. J., 2003, *Calculation of UV attenuation and colored dissolved organic matter absorption spectra from measurements of ocean color*, J. Geophys. Res., 108 (C9), 3301, doi:10.1029/2000JC000514.

Kahru M., 1997, *Using satellites to monitor large-scale environmental change: A case study of cyanobacteria blooms in the Baltic Sea*, [in:] M. Kahru & C. W. Brown (eds.), *Monitoring algal blooms: New techniques for detecting large scale environmental change*, Springer-Verl. Land. Biosci., 43–61.

Kahru M., Mitchell B. G., 1999, *Empirical chlorophyll algorithm and preliminary SeaWiFS validation for the California Current*, Int. J. Remote Sens., 20, 3421–3429.

Kahru M., Mitchell B. G., 2001, *Seasonal and non-seasonal variability of satellite derived chlorophyll and colored dissolved organic matter concentration in the California Current*, J. Geophys. Res., 106 (C2), 2517–2529.

Kahru M., Savchuk O. P., Elmgren R., 2007, *Satellite measurements of cyanobacterial bloom frequency in the Baltic Sea: interannual and spatial variability*, Mar. Ecol.-Prog. Ser., 343, 15–23.

Kowalczuk P., 1999, *Seasonal variability of yellow substance absorption in the surface layer of the Baltic Sea*, J. Geophys. Res., 104 (C12), 30047–30058.

Kowalczuk P., Darecki M., Olszewski J., Kaczmarek S., 2005, *Empirical relationships between Coloured Dissolved Organic Matter (CDOM) absorption and apparent optical properties in Baltic Sea waters*, Int. J. Remote Sens., 26 (2), 345–370.

Kowalczuk P., Kaczmarek S., 1996, *Analysis of temporal and spatial variability of yellow substance absorption in the Southern Baltic*, Oceanologia, 38 (1), 3–32.

Kowalczuk P., Sagan S., Olszewski J., Darecki M., Hapter R., 1999, *Seasonal changes in selected optical parameters in the Pomeranian Bay in 1996–1997*, Oceanologia, 41 (3), 309–334.

Kowalczuk P., Stedmon C. A., Markager S., 2006, *Modeling absorption by CDOM in the Baltic Sea from season, salinity and chlorophyll*, Mar. Chem., 101 (1–2), 1–11.

Kutser T., 2004, *Quantitative detection of chlorophyll in cyanobacterial blooms by satellite remote sensing*, Limnol. Oceanogr., 49 (6), 2179–2189.

Kutser T., Paavel B., Metsamaa L., Vahtmäe E., 2009, *Mapping coloured dissolved organic matter concentration in coastal waters*, Int. J. Remote Sens., 30 (22), 5843–5849.

Mannino A., Russ M. E., Hooker S. B., 2008, *Algorithm development and validation for satellite-derived distributions of DOC and CDOM in the U.S. Middle Atlantic Bight*, J. Geophys. Res., 113, C07051, doi:10.1029/2007JC004493.

Maritorena S., Siegel D. A., Peterson A. R., 2002, *Optimization of of a semi-analytical ocean color model for global-scale applications*, Appl. Optics, 41 (15), 2705–2714.

Melin F., Maritorena S., 2007, *Data merger success criteria*, [in:] *Ocean colour data merging*, W. Gregg (ed.), IOCCG Rep. No. 6, Dartmouth, CA, 68 pp.

Morel A., Gentili B., 1993, *Diffuse reflectance of oceanic waters, II Bidirectional aspects*, Appl. Optics, 32 (33), 6864–6872.

Morel A., Prieur L., 1977, *Analysis in variation of ocean color*, Limnol. Oceanogr., 22 (4), 709–722.

Moses W. J., Gitelson A. A., Berdnikov S., Povazhniy V., 2009, *Estimation of chlorophyll-a concentration in case II waters using MODIS and MERIS data-successes and challenges*, Environ. Res. Lett., 4, 045005, doi:10.1088/1748 -9326/4/4/045005, 8 pp.

Mueller J. L., Austin R. W., 1992, *Ocean optics protocols for SeaWiFS validation*, NASA Tech. Memo. 104566, Vol. 5, NASA Goddard Space Flight Center, Greenbelt, MD, 43 pp.

Olszewski J., Sagan S., Darecki M., 1992, *Spatial and temporal changes in some optical parameters in the southern Baltic*, Oceanologia, 33, 87–103.

Olszewski J., Sokólski M., Kuśmierczyk-Michulec J., 1995, *The method of continuous measurements of the diffusivity of the natural light field over the sea*, Oceanologia, 37 (2), 299–310.

O'Reilly J. E., Maritorena S., Mitchell B. G., Siegel D. A., Carder K. L., Garver S. A., Kahru M., McClain C. R., 1998, *Ocean color algorithms for SeaWiFS*, J. Geophys. Res., 103 (C11), 24937–24953.

Reinart A., Kutser T., 2006, *Comparison of different satellite sensors in detecting cyanobacterial bloom events in the Baltic Sea*, Remote Sens. Environ., 102 (1–2), 74–85.

Ruddick K. G., Ovidio F., Rijkeboer M., 2000, *Atmospheric correction of SeaWiFS imagery for turbid coastal and inland waters*, Appl. Optics, 39 (6), 897–912.

Sagan S., 1991, *Light transmission in the water of the southern Baltic Sea*, Diss. Monogr. 2, Inst. Oceanol. PAN, Sopot, 137 pp., (in Polish).

Sagan S., 2008, *The inherent optical properties of Baltic waters*, Diss. Monogr. 21, Inst. Oceanol., Sopot, 244 pp., (in Polish).

Sathyendranath S. (ed.), 2000, *Remote sensing of ocean colour in coastal, and other optically-complex, waters*, IOCCG Rep. No. 3, Dartmouth, CA, 140 pp.

Siegel H., Gerth M., Ohde T., Heene T., 2005, *Ocean colour remote sensing relevant water constituents and optical properties of the Baltic Sea*, Int. J. Remote Sens., 26 (2), 315–334.

Siegel D. A., Maritorena S., Nelson N. B., Behrenfeld M. J., 2005a, *Independence and interdependencies among global ocean color properties: Reassessing the bio-optical assumption*, J. Geophys. Res., 110, C07011, doi:10.1029/2004JC002527.

Siegel D. A., Maritorena S., Nelson N. B., Behrenfeld M. J., McClain C. R., 2005b, *Colored dissolved organic matter and its influence on the satellite-based characterization of the ocean biosphere*, Geophys. Res. Lett., 32, L20605, doi:10.1029/2005GL024310.

Siegel D. A., Maritorena S., Nelson N. B., Hansell D. A., Lorenzi-Kayser M., 2002, *Global distribution and dynamics of colored dissolved and detrital organic materials*, J. Geophys. Res., 107 (C12), 3228, doi:10.1029/2001JC000965.

Sverdrup H. U., 1953, *On conditions for the vernal blooming of phytoplankton*, J. Cons. Cons. Int. Explor. Mer., 18 (3), 287–295.

Zibordi G., Ferrari G. M., 1995, *Instrument self-shading in underwater optical measurements: Experimental data*, Appl. Optics, 34 (2), 2750–2754.